Multivariate Network Analysis of NIRS and Systemic Signals of Neonates following Birth Asphyxia

Markus Ferdinand Dablander

UCL CoMPLEX MRes Project Report 1

Project Supervisors:

Dr. Tachtsidis Ilias
University College London

Dr. Subhabrata Mitra
University College London

August 19, 2017

Abstract

NIRS- and systemic signals from neonates following birth asphyxia are analyzed by performing network transformation via the horizontal visibility algorithm. For each neonate ($n = 25$), the multivariate signal is transformed into a multilayer network. The topological properties of each multilayer network are investigated by computing different structural descriptors from mathematical graph theory. These structural descriptors provide quantification methods for signal analysis concepts like correlation, independence and entropy. Statistical tests are applied to detect significant differences in these descriptors between neonates with mild ($n_m = 13$) and neonates with severe ($n_s = 12$) brain injury. Significant discrepancies between the two goups were found for the signals for HbD, $tcpO_2$ and SpO_2. Among other things, the severely injured group showed a decreased correlation between HbD and $tcpO_2$, a higher independence between SpO_2 and $tcpO_2$ and a higher entropy for $tcpO_2$. Attempts are made to biologically interpret the result within the medical context of birth asphyxia. Future research directions are discussed, as well as possible applications of network analysis for brain injury classification.

Contents

Word Count: 6427

1 Introduction

1.1 Birth Asphyxia and the Problem of Early Brain Injury Classification

Neonatal injury due to oxygen deprivation during birth is referred to as birth asphyxia. Birth asphyxia occurs in about 1 in 1000 births and is strongly linked to hypoxic-ischaemic encephelopathy (HIE), a condition where a lack of oxygen due to reduced blood flow causes damage to the brain (Vannucci, [2000], [15]). This damage can cause partial failure of cerebral autoregulation [1] as well as dramatic neurodevelopmental impairment resulting in long-term disability or, in severe cases, death.

Infants that are suspected of having suffered from birth asphyxia are usually treated by whole body hypothermia (around 33 degrees Celsius); this has the potential to reduce the risk of death and impairment (Shankaran et al.,[2005], [13]).

To be able to detect neonates at risk and make fast decisions about which infants should undergow hypothermia and other treatment methods, there is a strong need to assess brain damage severity as soon as possible. What is needed is a reliable and safe method of brain injury classification right after birth. Taking the possible instability of certain infants after birth into account, this method should not only be fast but also as gentle as possible and it should be measurable at the bedside.

So far, there are multiple techniques available to measure the severity of HIE in neonates, which include measurements obtained via electroencephelography (EEG), magnetic resonance imaging (MRI), magnetic resonance spectroscopy (MRS) and near-infrared spectroscopy (NIRS). Most of these techniques, however, have either not been sufficiently reliable or sufficiently easy to apply. This study focusses on a new approach involving network analysis of NIRS and systemic signals.

1.2 Research Objectives and Review of Analysis Methods

NIRS measurements of brain tissue and standard systemic signals are comparatively easy and fast to obtain and it is reasonable to assume that these measurements contain information about the degree of brain injury. However, sophisticated signal analysis methods are needed in order to be able to analyze the data in a way that allows classification of the neonates according to the severity of their injury; but how to process the NIRS and systemic signals in order to reach this ambitious goal is still an open field of research and there is a need for experimentation with different analysis techniques in order to get a deep understanding of the medical data.

[1] Cerebral autoregulation (CA) is the ability of the brain to maintain stable blood flow, in spite of changing perfusion pressure. It is a biological mechanism to protect the brain from hypoperfusion and hyperperfusion.

A variety of signal processing techniques has already been developed to analyze and classify clinical data obtained via NIRS and systemic measurements in different medical settings.

Caicedo et al. [2016] [2] assumed a linear dependency of NIRS signals on systemic signals and then presented an algorithm (SIDE-ObSP) to decompose the NIRS signal into additive components of systemic data using *obique subspace projections*, a technique from linear algebra that generalizes orthogonal projections on linear subspaces. The SIDE-ObSP algorithm decomposes the NIRS signal such that each component corresponds to the linear influence of one specific systemic signal. This allows interesting medical interpretations, especially when it comes to assessing the state of cerebral hemodynamic regulation mechanisms, which might be impaired in neonates with birth asphyxia. In a case study using systemic and NIRS data from 20 neonates during the first 3 days of life, SIDE-ObSP could successfully decouple the influence of changes in arterial oxygen saturation from the NIRS measurements, which allowed the use of NIRS signals as an approximate measure for cerebral blood flow.

Bale et al. [2014] [1] used NIRS and mean arterial blood pressure (MABP) measurements to investigate the relationship between cerebral autoregulation and the neurotoxic effects of anaesthesia in newborn piglets. As a marker for impaired cerebral autoregulation, they used concordance between MABP and intravascular oxygenation (HbD); this concordance was quantified by performing *coherence analysis* between MABP and HbD. Under certain restrictions, the coherence between two signals provides a measure for the linear dependency between those signals over a certain time span. They could show that concordance of MABP and HbD was significantly higher in those piglets that had received minor surgery during anaesthesia compared to a group of piglets that had received anaesthesia without surgery.

Kleiser et al. [2016] [5] used *maximum entropy spectral analysis* and *recurrence quantification analysis*, two techniques from nonlinear dynamical systems theory, to characterize the fluctuations and interrelationships of arterial tissue oxygen saturation (SpO_2), cerebral tissue oxygen saturation (StO_2), heart rate (HR) and fractional tissue oxygenation extraction (FTOE) in NIRS and systemic signals obtained from four preterm neonates. Amongst other results, they found that the nonlinear correlation strength between FTOE and HR showed a higher value for neonates with a reduced health status, which could indicate deficiencies in cerebral autoregulation.

Highton et al. [2015] [4] studied the relationship between NIRS signal oscillations and multimodal neuromonitoring in a total number of 27 sedated, ventilated, brain-injured patients by using *wavelet measures of phase and coherence*. They concluded that these analysis methods have the potential to provide accurate measures for the state of cerebral autoregulation, but only when combined with prior physiological knowledge

Rowley et al [2006] [11] applied *wavelet cross-correlation* to quantify the relationship between low-frequency oscillations in cerebral oxyhemoglobin (O_2Hb) and MABP in patients with failure of the sympathetic nervous system and a control group and found statistically significant differences. They proposed that

wavelet cross-correlation can serve as a method to assess the state of cerebral autoregulation and emphasized the advantage of not having to assume stationarity of the underlying time series for this technique.

The goal of this project is to experiment with the application of a novel analysis technique to medical data from neonates with birth asphyxia; a method that transforms multivariate time series into networks. The specific objectives are

- to apply *mulitvariate network analysis via the horizontal visibility algorithm* to NIRS and systemic signals from neonates suffering from birth asphyxia,
- to investigate, whether multivariate network analysis is able to detect significant differences between neonates with mild and severe brain injury and, where possible,
- to give potential biological interpretations for the results.

Differences in the medical signals of healthy and injured infants can both stimulate new biological insights and guide the way for the further development of a brain injury classifier that is solely based on the analysis of NIRS and systemic signals.

In the following sections we are going to discuss the available measurements and then give a detailed description of the analysis method. This description is followed by a discussion of the results as well as a critical examination of the data, our method and possible future research directions.

2 Data: One Multivariate Time Series per Baby

Our data consists of brain tissue physiology signals obtained via NIRS as well as standard systemic signals for $n = 25$ infants with birth asphyxia. The measurements were taken between 2014 and 2015 at the neonatal intensive care unit (NICU) at UCL Hospital (UCLH).

For each infant, we are looking at a multidimensional time series consisting of 1 measurement per second for a time span between 2189 and 3621 seconds [2]. Each time series is composed of the following 7 signals:

- Cytochrome-c-oxidase (CCO) [uM]
- Cerebral total hemoglobin (HbT) [uM]
- Hemoglobine difference (HbD) [uM]
- Arterial oxygen saturation (SpO_2) [%]
- Transcutaneous oxygen ($tcpO_2$) [kPa]
- Transcutaneous carbon dioxide ($tcpCO_2$) [kPa]
- Heart Rate (HR) [bpm]

Each measurement was taken within the first 4 days of birth with the majority of them being taken at day 2 and 3. [3]

In a second step, movement artefacts were reduced using the method proposed by Scholkmann [2010] [12].

After this, the 25 data sets were split up according to the severity of brain injury. This splitting was done by making use of an available biomarker that was found to have predictive power over future neurodevelopmental impairment (Penrice et al. [1996] [10]): the *lactate/N acetyl aspartate (Lac/NAA) ratio.*

The Lac/NAA ratio is measured via MRS; it is not easily obtained and cannot be measured until about 1 week after birth. Penrice et al. observed that healthy newborns have a Lac/NAA ratio < 0.3 while newborns with severe brain injury have a ratio > 0.3. This gives a threshold to divide the neonates into two groups. These two groups will be referred to as the *mild* group ($n_m = 13$) and the *severe* group ($n_s = 12$).

Below we can see the plots of the 7 signals of an example data set obtained from a neonate with Lac/NAA ratio of 0.39. The plots were created using the `Python` library `Pyplot`. The first three plots show the NIRS signals (CCO, HbD,

[2] Only two "short" signals had lengths of 2189 and 3079 seconds, the other 23 signals all had a length between 3619 and 3621 seconds

[3] One should note that data from different days can be clinically different; furthermore, most (but not all) of the babies in the data set had already received hypothermic treatment before the time of measurement. In this study, we will not take these differences into account due to the small available sample size; in a sufficiently large data set, however, it would be desirable to split the data up according to day of measurement and hypothermic treatment.

HbT), while the last four plots show the systemic signals (HR, SpO_2, $tcpO_2$, $tcpCO_2$).

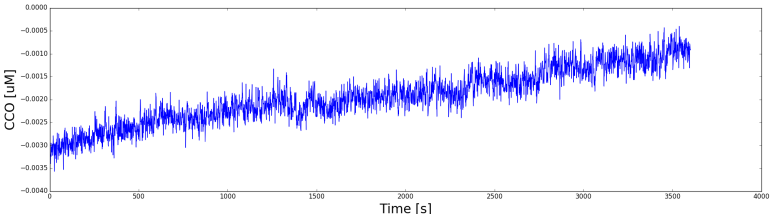

Figure 1: CCO (example)

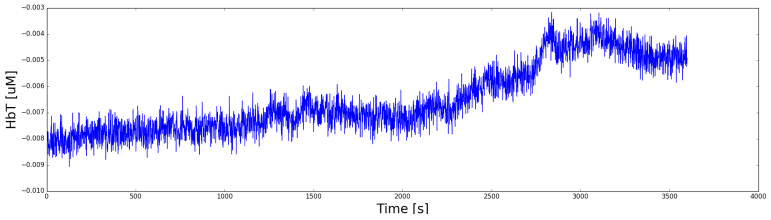

Figure 2: HbT (example)

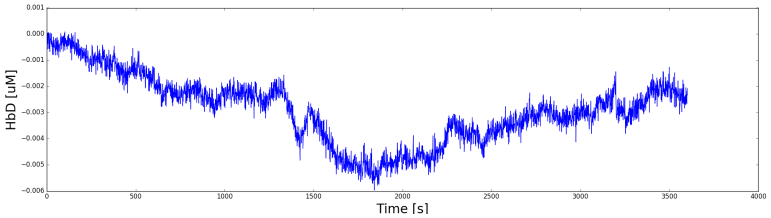

Figure 3: HbD (example)

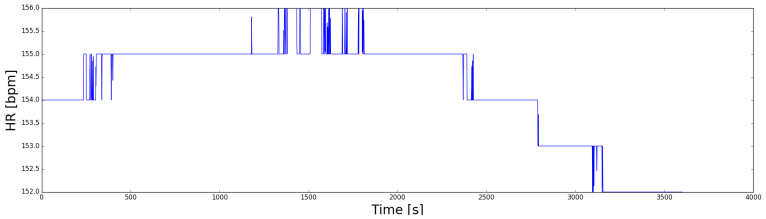

Figure 4: HR (example)

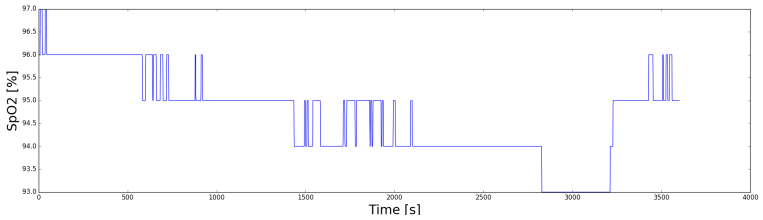

Figure 5: SpO_2 (example)

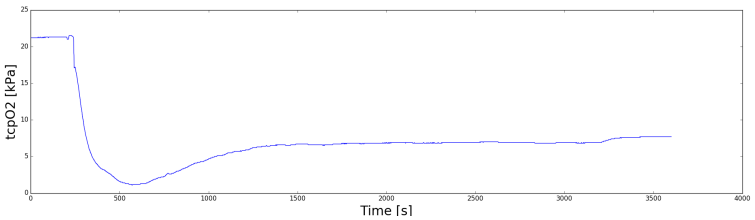

Figure 6: $tcpO_2$ (example)

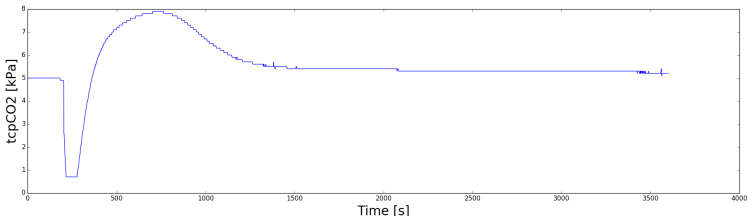

Figure 7: $tcpCO_2$ (example)

Even though no certain conclusions can be drawn solely from looking at the plots, it is interesting that HbD and SpO_2 appear to be somewhat correlated in this example. We know that the Lac/Naa ratio of this newborn indicates severe injury. Could this coherence between HbD and SpO_2 possibly be somehow linked to failure of cerebral autoregulation? Advanced data analysis methods are needed to look for patterns in the data.

3 Method: Transformation of Multidimensional Time Series to Networks

3.1 The Horizontal Visibility Algorithm

The horizontal visibility algorithm (HVA) provides a way to transform one-dimensional (and then multidimensional) time series into static networks. There are many different ways to transform time series data into networks; the advantage of the HVA is that it is both simple enough to be easily applicable and sopisticated enough to be able to extract interesting information. In many cases, the HVA is able to preserve key features of the dynamic of the underlying time series and encode these features in the structure of the resulting network; it has recently attracted the interest of a growing number of researchers and the number of its theoretical and practical applications is growing.

Lacasa et al. [2014] [6] have summarized the most important information about using the HVA for the analysis of time series data. As an example, they applied the HVA to financial data and showed that it can efficiently discriminate crises from periods of financial stability. Luque et al. [2009] [8] as well as Lacasa and Toral [2010] [7] have pointed out, that the HVA is a suitable tool to distinguish whether a given time series is produced by a chaotic deterministic or by a random process. Stephen [2015] [14] has applied the HVA to analyze time series data from pedestrian trajectories in public places and has shown that the resulting networks can accurately reflect clustering as well as global dynamics within a crowd of people. So how does the HVA work?

The mathematical formalization of a network is called a *graph*[4]. A (finite, simple) graph $G = (V, E)$ consists of a set of vertices $V = \{1, ..., n\}$ and a set of edges between those vertices $E \subseteq \{\{i, j\} \mid i, j \in V, i \neq j\}$. There is an edge between two different vertices i and j if and only if $\{i, j\} \in E$.

Graphs can easily be visualized by drawing a point for every vertex $i \in V$ and by drawing a line between all vertices i and j that are connected by an edge $\{i, j\}$.

Let us now consider a finite time series $x_1, ..., x_n$ with $x_i \in \mathbb{R}$. The HVA starts by constructing one vertex for each time point, which leaves us with a set $V = \{1, ..., n\}$ of vertices. We then add an edge between two different vertices $i, j \in V$ with $i < j$ if and only if

$$\min(\{x_i, x_j\}) \geq \max(\{x_{i+1}, ..., x_{j-1}\}).$$

So if we fix two values x_i and x_j, then there is an edge between i and j exactly if all values between x_i and x_j are both smaller than x_i and x_j. In the special case of $j = i + 1$, the set $\{x_{i+1}, ..., x_{j-1}\}$ is empty; in this case we also construct an edge between i and j, which means that neighbouring time points are always connected.

[4]The *graphs* that are studied in the field of graph theorie are abstract formalizations of networks and should not be confused with graphs of functions. In this paper, the terms *graph* and *network* are being used synonymously

Example 1 (HVA)**.** Let us consider a simple time series that was presented by Luque et. al. [2009] [8] to illustrate the HVA. It is depicted in figure 8.

We have 20 different values; this implies that our associated graph has 20 vertices $V = \{1, ..., 20\}$. Each vertex corresponds to one value and one point in time. We construct an edge between 1 and 2, since they are neighbouring time points. Furthermore, there is no value between 0.71 and 0.56 that is bigger than either 0.71 or 0.56, so we construct an edge between vertex 1 and vertex 3. But we do not connect vertices 1 and 4 by an edge since there are values between 0.71 and 0.29 that are bigger than 0.29. Proceeding like this, we obtain the graph shown in the lower part of figure 1. A graph constructed from a time series via the HVA is referred to as *horizontal visibility graph*.

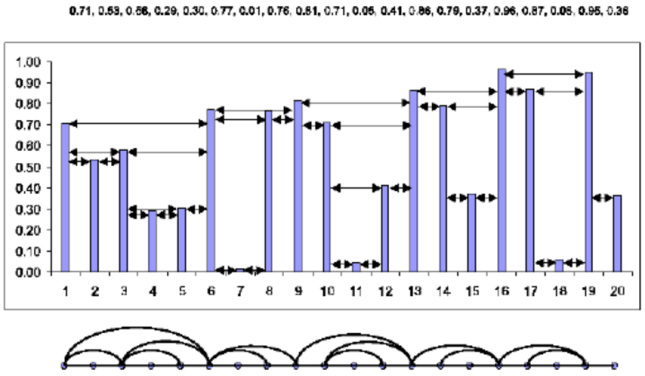

Figure 8: Illustration of the HVA for a short time series of length $n = 20$. (Source: [8, p. 3])

Using the programming language `Python` and the numerical library `Numpy` (as `np`), one can easily implement a function `network(ts)` that transforms a time series into a graph via the HVA. The input of this function is a 1-dimensional array

$$ts = [x_1, x_2, ..., x_n]$$

containing the timeseries. The output is a square matrix G of dimension n that only contains the integers 0 and 1. There is an edge between i and j if and only if $G(i, j) = 1$ and otherwise $G(i, j) = 0$. G is also called the *adjacency matrix* of the graph.

```
#Horizontal Visibility Algorithm in Python

def network(ts):
  n = len(ts)
  A = np.zeros((n,n),int)
  for i in range(0,n-1):
    for j in range(i+1,n):
      if j == i+1:
        A[i,j] = 1
      elif j > i+1:
        if np.amax(ts[i+1:j]) < np.amin([ts[i],ts[j]]):
          A[i,j] = 1
      if ts[j] >= ts[i]:
        break
   G = A + np.transpose(A)
return G
```

We can also generalize the HVA to deal with multidimensional time series. To do this, we interpret any k-dimensional time series

$$(x_{11}, ..., x_{1k}), ..., (x_{n1}, ..., x_{nk})$$

as k different 1-dimensional time series

$$x_{1i}, .., x_{ni}, \qquad i \in \{1, ..., k\},$$

by "reading" the k-dimensional vectors $(x_{11}, ..., x_{1k}), ..., (x_{n1}, ..., x_{nk})$ componentwise. Then one can apply the HVA to the resulting 1-dimensional time series to transform the multidimensional signal to a total number of k different networks, each network corresponding to one component of our multidimensional signal. The k networks are often interpreted as one big *multilayer network*, where the networks are imagined to be built on top of each other like the floors of a building.

Figure 9 shows a multilayer network that was constructed by transforming a 3-dimensional time series with 10 values. The figure was made with `Python` by using the multilayer network library `Pymnet`. Each layer consists of one network and each network corresponds to one 1-dimensional component of the original 3-dimensional time series.

After the transformation, one can start to investigate the properties of the original k-dimensional time series by both studying the structures of the graphs that belong to each component and by studying the interrelationships between these graphs in the multilayer network to to get insights into the relationships between the signals of which the multimodal time series is composed of. A powerful way to characterize graphs and relationships between pairs of graphs is by computing and analyzing *structural descriptors*.

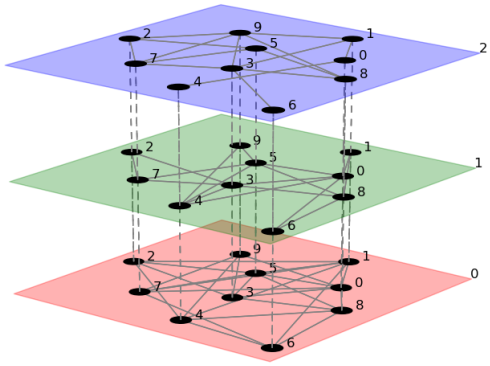

Figure 9: Multilayer network constructed from a 3-dimensional time series of length 10.

3.2 Structural Descriptors

A structural descriptors is a single numbers that is assigned to a given graph (or a set of graphs) to describe its properties. There is a wide range of different structural descriptors, that are all constructed in different ways and that focus on different aspects of the graph at hand.

In this section, we will shortly define and discuss the structural descriptors that were used in this study. Where possible, we will also try to find intuitive interpretations for the descriptors and think about what certain descriptor values of a horizontal visibility graph mean for its underlying time series.

- **Average Edge Overlap**: Let us consider two graphs G_1 and G_2 with an equal number of nodes n. Then the average edge overlap between G_1 and G_2 is defined via

$$w(G_1, G_2) := \frac{\sum_{i=1}^{n-1} \sum_{j=i+1}^{n} \delta_{G_1}(i,j) + \delta_{G_2}(i,j)}{2 \sum_{i=1}^{n-1} \sum_{j=i+1}^{n} \delta_{G_1,G_2}(i,j)}.$$

Here

$$\delta_G(i,j) := \begin{cases} 1 & \text{if there is an edge between } i \text{ and } j \text{ in } G \\ 0 & \text{otherwise} \end{cases} \tag{1}$$

and

$$\delta_{G_1,G_2}(i,j) := \begin{cases} 1 & \text{if there is an edge between } i \text{ and } j \text{ in } G_1 \text{ or } G_2 \\ 0 & \text{otherwise} \end{cases} \tag{2}$$

If we imagine G_1 and G_2 to be the layers of a 2-layer network, then the average edge overlap between two graphs is nothing but the expected fraction of layers on which a randomly chosen edge is going to appear. One can show that $w(G_1, G_2)$ is always between $1/2$ and 1. If $w(G_1, G_2) = 1/2$, then no edge in our 2-layer network appears on both layers. If $w(G_1, G_2) = 1$, then every edge in our 2-layer network appears on both layers.

If we think in terms of signals, then a high average edge overlap between the two horizontal visibility graphs of two 1-dimensional time series is a sign of high correlation between those two signals. Lacasa et al. [2014] [6] have already noted, that the average edge overlap of a 2-layer horizontal visibility graph can be interpreted as an approximation for the overal coherence of the original 2-dimensional time series, where high values of $w(G_1, G_2)$ indicate high correlation of both signals. Due to its general construction, the average edge overlap is suitable to detect both linear and nonlinear correlations.

- **Entropy of Degree Distribution:** The degree of a vertex $v \in V$ of a graph G with n vertices is the number of edges in G that are directly linked to v. If we now randomly choose a vertex v in G, then the probability that v has degree k is given via

$$P_G(k) := \frac{\text{Number of Vertices in G with Degree k}}{\text{Total Number n of Vertices in G}}.$$

The function P_G is referred to as the degree distribution of the graph G. Since P_G is a discrete probability distribution, we can easily compute its *Shannon entropy* (or just *entropy*) via

$$H(P_G) := -\sum_{k=0}^{n-1} P_G(k) \log(P_G(k))$$

The entropy $H(P_G)$ is a measure for our uncertainty about the degree of a randomly chosen vertex in G. Generally speaking, the higher the entropy of a random experiment, the less foreseeable the outcome is if we know nothing but the probability distribution of this experiment.

If G is a horizontal visibility graph constructed from a 1-dimensional time series, then high values of $H(P_G)$ indicate irregular and non-repetitive behaviour of the signal, while low values of $H(P_G)$ indicate a tendency towards periodicity and regularity.

- **Mutual Information of Degree Distributions** We now look at two different graphs G_1 and G_2 on the same set of vertices $V = \{1, ..., n\}$. We can interpret these two graphs as two layers of a multilayer network. In addition to the degree distributions P_{G_1} and P_{G_2}, we define the joint degree distribution P_{G_1,G_2} via

$P_{G_1,G_2}(k_1, k_2) := P(\text{Chosing a vertex with degree } k_1 \text{ in } G_1 \text{ and } k_2 \text{ in } G_2)$

$P_{G_1,G_2}(k_1, k_2)$ can easily be computed numerically for two given graphs of reasonable size. Now the mutual information between both degree distributions is defined by

$$I(G_1, G_2) := \sum_{k_1=0}^{n-1} \sum_{k_2=0}^{n-1} P_{G_1,G_2}(k_1, k_2) \log(\frac{P_{G_1,G_2}(k_1, k_2)}{P_{G_1}(k_1) P_{G_2}(k_2)}).$$

In general, the mutual information of two random variables X and Y is a quantity from information theory that measures the *mutual dependence* of those two random variables. If the mutual information is very high, it means that knowing the value of X is very useful in predicting Y (and the other way round, since the mutual information is symmetric). In this study, we are going to use a normalized version of the mutual information that only takes values between 0 and 1.

If this normalized mutual information is 0, it implies independence between X and Y; if it is 1 it implies that at least one of the two random variables is completely determined by the other one.

In our case of horizontal visibility graphs, high mutual information between the degree distributions of the graphs of two signals can be interpreted as high dependence between those signals, while low mutual information implies that knowing one of the two signals does not tell us a lot about the other one.

Mutual information between degree distributions in a multilayer horizontal visibility network was successfully used by Lacasa et al. [2014] [6] to discriminate between turbulent close-to-independent and periodically synchronized qualitative behaviour in time series constructed from coupled chaotic maps. Mutual interlayer information could also accurately predict the onset of chaotic attractors with increasing interdependence of the 1-dimensional signals in such coupled chaotic systems.

Mutual information is a measure with the potential to detect complicated nonlinear dependencies in multivariate time series.

- **Transitivity:** A *triangle* with*in a gra*ph G is a set of three vertices in G that are all connected to each other. A *connected triple* in G is a set of three vertices in G where two vertices are connected to each other. Obviously, every triangle defines three connected triples. The transitivity of a graph is defined by

$$T(G) := \frac{3 * \text{Number of Triangles in } G}{\text{Number of connected triples in } G}$$

The transitivity is measure that cannot be interpreted easily in an intuitive way for horizontal visibility graphs of time series. It was used solely to detect abstract differences between the mild and the severe group in our study.

- **Assortativity:** The assortativity of a graph G is a measure for the correlation between the degrees of vertices of a graph that makes use of the Pearson correlation coefficient. It is a number between -1 and 1 and its exact mathematical definition as well as an interesting investigation of its properties can be found in a paper of Noldus and Van Mieghem [2015] [9].

  The assortativity quantifies the tendency of vertices to connect with vertices of the same degree. If assortativity is close to 1, them vertices of high degree tend to connect to vertices of high degree and vertices of low degree tend to connect to vertices of low degree. If assortativity is close to -1, on the other hand, then vertices of high degree are likely connected to vertices of low degree, and vice versa.

  Just like the transitivity of a graph. the assortativity of a horizontal visibility graph cannot be interpreted directly with respect to the underlying time series and it was used in this study solely to detect abstract differences within our two groups.

4 Results of Network Analysis

4.1 Significant Structural Descriptors and Interpretation

For each of the $n = 25$ available multivariate time series, `Python` was used to generate a 7-layer network via the horizontal visibility algorithm. One baby corresponds to one 7-layer multinetwork.

In section 2 we plotted the signals for a neonate with a Lac/NAA ratio of 0.39; the network transformations of the first 600 seconds of each of these signals can now be seen in figures $10 - 16$.

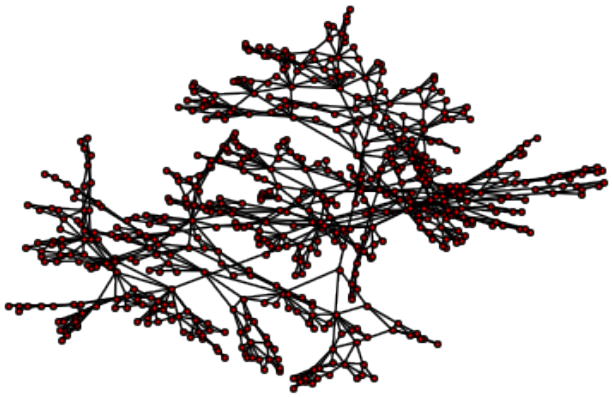

Figure 10: Network Transformation (CCO-signal, 600 seconds)

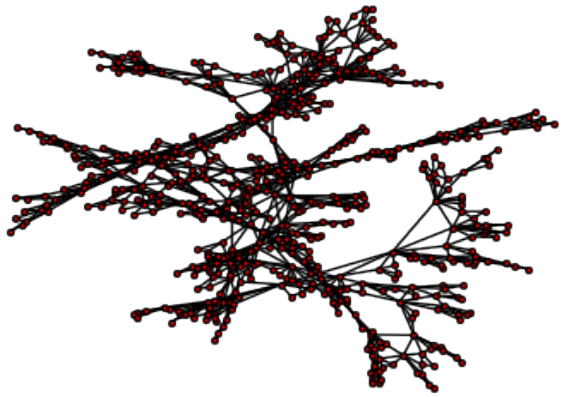

Figure 11: Network Transformation (HbT-signal, 600 seconds)

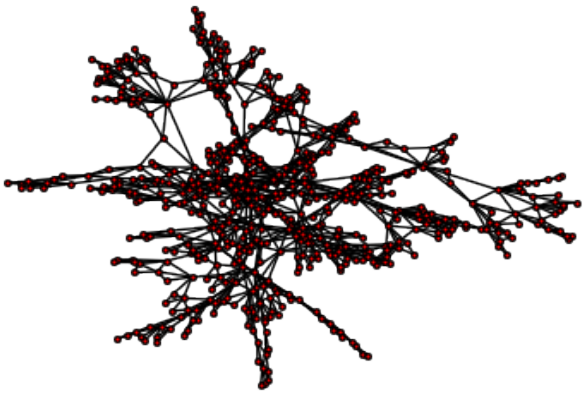

Figure 12: Network Transformation (HbD-signal, 600 seconds)

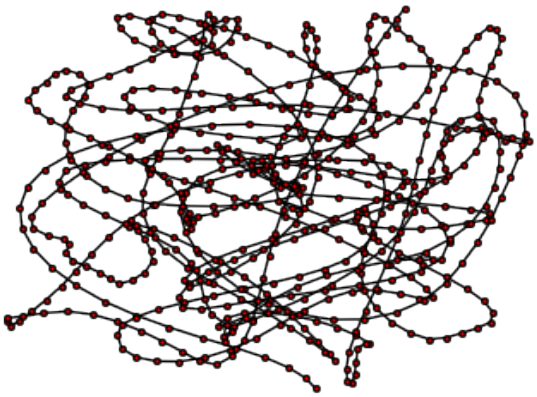

Figure 13: Network Transformation (HR-signal, 600 seconds)

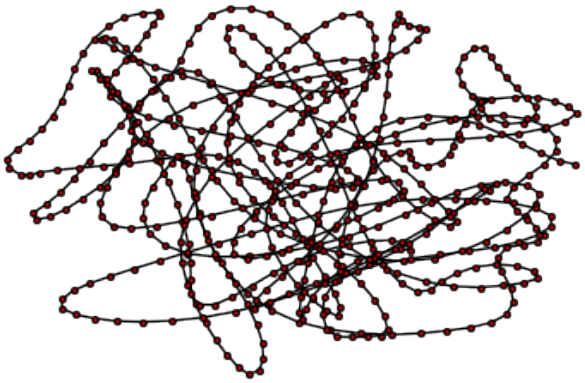

Figure 14: Network Transformation (SpO_2-signal, 600 seconds)

Figure 15: Network Transformation (tcpO_2-signal, 600 seconds)

Figure 16: Network Transformation (tcpCO_2-signal, 600 seconds)

There is a clear visual difference between the networks of NIRS signals and the networks of systemic signals, which can partly be explained by the lower fluctuations of systemic signals. Since systemic signals are often approximately constant over short time intervals, their networks get a more rope-like structure, while the fast fluctuations of NIRS signals lead to more complicated and irregular patterns.

After the network transformation, all of the structural descriptors discussed in section 3 were computed for each multilayer network. One 7-layer network can be used to calculate 7 times the entropy of the degree distribution, 7 transitivities, 7 assortativities, 21 average edge overlaps and 21 times the mutual information of degree distribution; this left us with a total number of 63 structural descriptors to compute per baby.

For each of those 63 structural descriptors, both the Anderson-Darling and the Kolmogorow-Smirnow test were applied to look for differences between the mild group ($n_m = 13$) and the severe group ($n_s = 12$).

Significant statistical differences [5] were found for the following 7 descriptors:

- Average Edge Overlap: (HbD, tcpO_2)
- Average Edge Overlap: (SpO2, tcpO_2)
- Normalized Mutual Information: (SpO2, tcpO2)
- Entropy of Degree Distribution: tcpO_2
- Assortativity: HbD
- Assortativity: tcpO_2
- Transitivity: HbD

On the next pages, we are going to plot and interpret the most interesting of these results: the significant differences in average edge overlap, mutual information and entropy of degree distribution.

The differences in assortativity and transitivity are clearly significant, but of abstract nature and it is very difficult to directly see their relationships to their underlying signals. This is why we will not further discuss them here. But the fact that we were able to detect differences in these two descriptors within our groups is encouraging, since it supports the view that our signals carry the essential information to distinguish between mild and severe cases of birth asphyxia. Furthermore, in a future scenario with more available data, these abstract quantities could turn out to be extremely valuable for feature engineering in a directed machine learning approach.

[5] All results had p-values < 0.03 for both tests.

Average Edge Overlap: (HbD, tcpO$_2$)

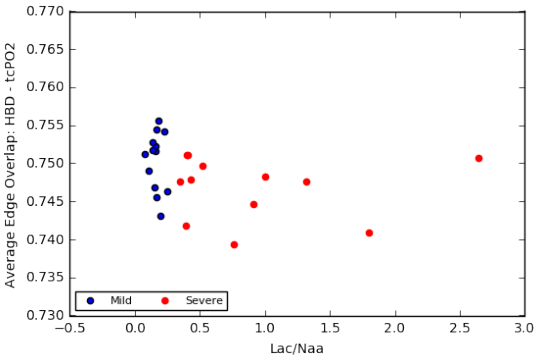

Figure 17: Scatterplot Overlap (HbD, tcpO$_2$)

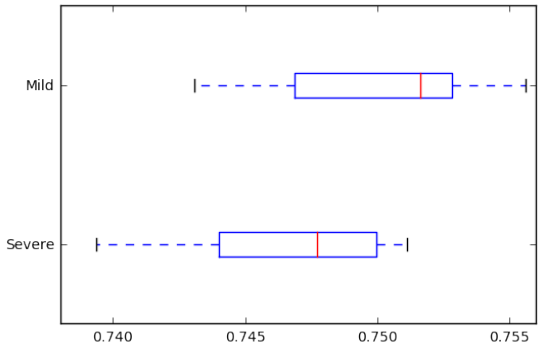

Figure 18: Boxplot Overlap (HbD, tcpO$_2$)

The severe group has a lower mean average edge overlap between HbD and tcpO$_2$ (0.747 compared to 0.750). This indicates a lower correlation between HbD and tcpO$_2$ for severe cases.

HbD serves as an indirect marker for cerebral blood flow and the systemic tcpO$_2$ measurement reflects oxygen delivery to the tissue. Therefore, a lower correlation between these signals for the severe group seems contradictory at first sight to our expectation of impaired cerebral autoregulation; impaired cerebral autoregulation would intuitively lead us to expect a high correlation between HbD and tcpO$_2$.

It is possible though, that the results can be explained with the occurrence of *secondary energy failure* in the cerebral tissue of severe cases. Secondary energy failure describes the phenomenon of a second drop in cerebral blood flow several days after the initial oxygen deprivation (Hassel et al. [2015], [3]). If we assume, that this drop in cerebral oxygen supply happens, to some extent,

independently of the value of $tcpO_2$, then it is imaginable, that there is a low to moderate correlation between HbD and $tcpO_2$ in healthy infants with intact autoregulation and that this low correlation is further reduced in severely injured infants who experience secondary energy failure.

Average Edge Overlap: (SpO_2, $tcpO_2$)

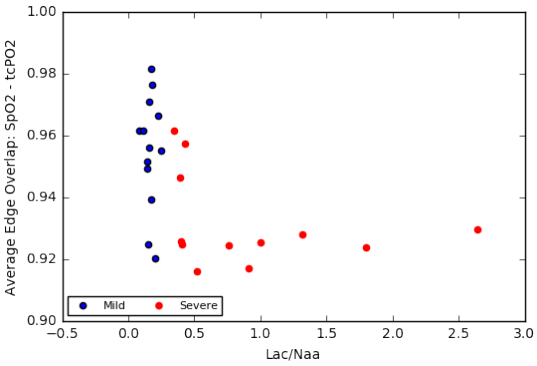

Figure 19: Scatterplot Overlap (SpO_2, $tcpO_2$)

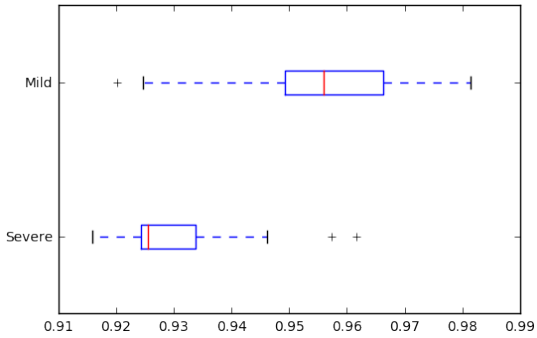

Figure 20: Boxplot Overlap (SpO_2, $tcpO_2$)

It does not come as a surprise, that the average edge overlap of SpO_2 with $tcpO_2$ is close to the maximum value of 1 in both groups, since SpO_2 [%] measures the blood oxygen saturation and $tcpO_2$ measures oxygen supply to the tissue. This result describes a relationship between two purely systemic signals.

The severe group has a lower mean average edge overlap between SpO_2 and $tcpO_2$ (0.932 compared to 0.955). This is a sign for decreased correlation between those signals. This could possibly indicate a reduced ability of the organism to properly deliver available oxygen from the blood to the tissue.

If this is indeed the case, however, it remains to clarify if and how such a condition can be linked to brain injury. It could be that there is no causal relation between brain injury and reduced ability to deliver blood oxygen to the tissue; this reduced ability could instead be the result of a third condition linked to or caused by birth asphyxia.

Most investigations concerning birth asphyxia focus on brain injury, due to the dramatic consequences of neuronal damage for a newborn. But hypoxic damage can occur to most of the organs (heart, lungs, liver, gut, kidneys); injury in one of these areas could have the potential to explain the above observations.

Normalized Mutual Information: (SpO_2, $tcpO_2$)

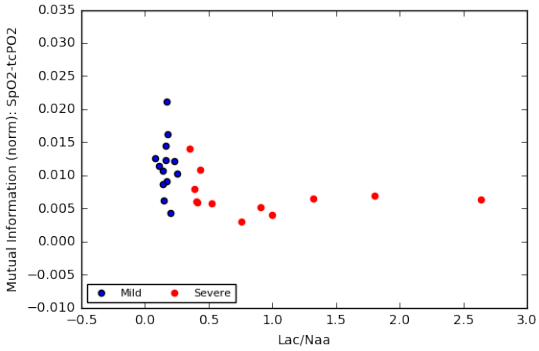

Figure 21: Scatterplot Mutual Information (SpO_2, $tcpO_2$)

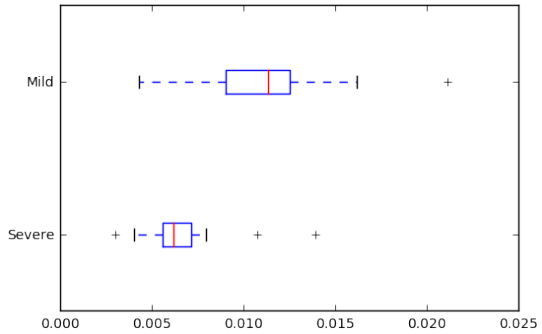

Figure 22: Boxplot Mutual Information (SpO_2, $tcpO_2$)

The severe group has a lower average mutual information between SpO_2 and $tcpO_2$ (0.007 compared to 0.0115), which is a sign for a reduced dependency between those signals. Both signals are more decoupled from each other. In the

severe group, knowing one of those signals tells us less about the other signal than in the mild group.

This can be seen as a more abstract version of the previous result; the result is likely at least partially caused by the reduced correlation between SpO_2 and $tcpO_2$ in the severe group (measured by the average edge overlap). The result points in the direction of a reduced dependency between blood oxygen levels and tissue oxygenation for neonates with severe brain injury.

We can also clearly observe a lower standard deviation of mutual information between SpO_2 and $tcpO_2$ within the severe group (0.00685 compared to 0.0115), which implies a higher similarity of the results in this group. It is imaginable that there are biological mechanisms active in healthy neonates that cause a natural fluctuation in the dependency of SpO_2 and $tcpO_2$; it might be that some of these mechanisms are damaged or lost in the severe group, causing this dependency to drop and get stuck on a stable and low level.

Entropy of Degree Distribution: $tcpO_2$

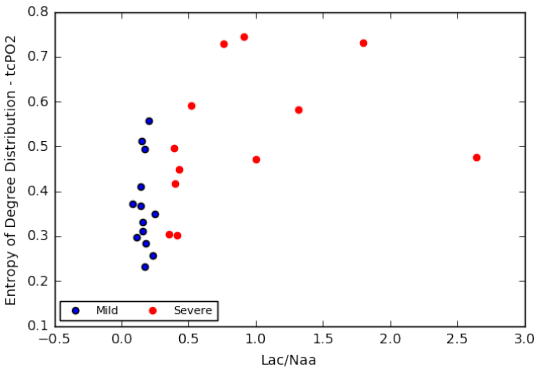

Figure 23: Scatterplot Entropy of Deg. $tcpO_2$

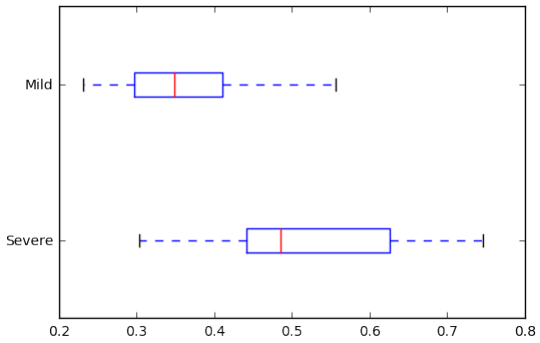

Figure 24: Boxplot Entropy of Deg. $tcpO_2$

The severe group has a significantly higher mean degree distribution entropy for the $tcpO_2$ network (0.367 compared to 0.525). This implies that brain injury due to birth asphyxia is linked to a more unpredictable and irregular tcpO2 signal. An irregular $tcpO_2$ signal in turn is a sign for irregular and fluctuating oxygen supply to the tissue.

Similar to the case of the average overlap between SpO_2 and $tcpO_2$, it might not be possible to find a direct causal link between this irregularity and neonatal brain injury. It is imaginable that general distress to the organism results in a more chaotic $tcpO_2$ signal; this distress could be caused by a variety of factors, including hypoxic damage to some systemic parts outside of the brain (heart, lungs) or secondary energy failure.

4.2 Discussion

The above results indicated that network analysis via the horizontal visibility algorithm is indeed capable of discriminating between the multimodal signals of infants with mild and severe brain injury. They are encouraging our view, that the data de facto carries the essential information needed to detect brain injury in neonates with birth asphyxia. Furthermore, the results stimulate the generation of biological hypotheses that could lead to valuable medical insights.

At this point, however, the differences found by our method were still too subtle to provide the opportunity to build a sufficiently reliable brain injury classification pipeline. This is most likely due to two obstacles.

The first obstacle is the unavoidable simplification of the signal happening during the network transformation. While researchers have observed that the horizontal visibility algorithm has the ability to catch much of the characteristic information contained in time series in different scenarios, it is not possible to uniquely reconstruct the original time series from the network, proving a certain unavoidable information loss. Without experiments involving a large enough data set, it is not possible to make a definite statement whether this information loss is negligible in the case of brain injury classification.

This leads to the second obstacle, which is the amount and length of the data. For many problems of a comparably high complexity, a sample size of $n = 25$ makes it hard to reach sufficient classification accuracy. Unfortunately, many of the signals discussed in this study are not easily obtained [6].

One should also note, that the length of an individual time series (in our study about 3600 seconds) has a major influence on its information content. It is imaginable, that some signals contain oscillations with a period that is too long to be properly reflected by one hour of measurement; but such oscillations might very well contain important information about the health status of the infant.

In a possible future sitution with more available data ($n >> 100$), the methods proposed in this report could turn out to be powerful and easily applicable tools to generate *features* in a classification approach via machine learning. The success of a machine learning classifier crucially depends on the scientific art of *feature engineering*[7], which is to find a way to drastically reduce the dimensionality of the data while catching as much essential information as possible. The structural descriptors that differed significantly between the mild and the severe groups are natural choices for such features and it would be very interesting to field test their predictive power.

Due to the fact that all significant results were connected to HbD, $tcpO_2$ and SpO_2, special emphasis should be put on those three signals in further analysis

[6] In spite of this, researchers at the neonatal intensive care unit (NICU) at UCL Hospital (UCLH) are steadily collecting data, creating an ever-growing and highly valuale set of measurements that is going to make this and other analysis approaches more and more powerful in the future.

[7] Feature engineering is sometimes referred to as an *art* rather than a science, because of the important role intuition plays in it; so far, there is no universal algorithm to find the best features in a general setting.

approaches.

The reduced correlation of HbD and $tcpO_2$ in the severe group calls for further investigations concerning the dependency of systemic oxygen delivery to the tissue and cerebral blood flow during secondary energy failure

Similarly, the lower mutual information between SpO_2 and $tcpO_2$ in the severe group calls for a deeper understanding of the dependency of these two systemic signals and how this dependency could be affected by birth asphyxia.

Future techniques could focus on applying different entropy measures to the $tcpO_2$ signal, since we have observed that this signal behaves more irregular in the severe group. A natural next step would be to apply techniques like *approximate entropy analysis* to get a deeper and clearer understanding of possible irregularities.

Finally, it would also be very interesting from a medical point of view to perform network analysis for CCO, HbD and mean arterial blood pressure (MABP) and to look for significant differences linked to brain injury severity. It is biologically reasonable that the relationships between these signals change when cerebral autoregulation is impaired. Network analysis for these signals will be performed by us in the close future.

References

[1] Gemma Bale, Aaron Oliver-Taylor, Igor Fierens, Kevin Broad, Jane Hassell, Go Kawano, Jamshid Rostami, Gennadij Raivich, Robert Sanders, Nicola Robertson, et al. Investigation of cerebral autoregulation in the newborn piglet during anaesthesia and surgery. In *Oxygen Transport to Tissue XXXVI*, pages 165–171. Springer, 2014.

[2] Alexander Caicedo, Carolina Varon, Borbala Hunyadi, Maria Papademetriou, Ilias Tachtsidis, and Sabine Van Huffel. Decomposition of near-infrared spectroscopy signals using oblique subspace projections: Applications in brain hemodynamic monitoring. *Frontiers in Physiology*, 7, 2016.

[3] K Jane Hassell, Mojgan Ezzati, Daniel Alonso-Alconada, Derek J Hausenloy, and Nicola J Robertson. New horizons for newborn brain protection: enhancing endogenous neuroprotection. *Archives of Disease in Childhood-Fetal and Neonatal Edition*, 100(6):F541–F552, 2015.

[4] David Highton, Arnab Ghosh, Ilias Tachtsidis, Jasmina Panovska-Griffiths, Clare E Elwell, and Martin Smith. Monitoring cerebral autoregulation after brain injury: multimodal assessment of cerebral slow-wave oscillations using near-infrared spectroscopy. *Anesthesia and analgesia*, 121(1):198, 2015.

[5] Stefan Kleiser, Marcin Pastewski, Tharindi Hapuarachchi, Cornelia Hagmann, Jean-Claude Fauchère, Ilias Tachtsidis, Martin Wolf, and Felix Scholkmann. Characterizing fluctuations of arterial and cerebral tissue oxygenation in preterm neonates by means of data analysis techniques for nonlinear dynamical systems. In *Oxygen Transport to Tissue XXXVII*, pages 511–519. Springer, 2016.

[6] Lucas Lacasa, Vincenzo Nicosia, and Vito Latora. Network structure of multivariate time series. *Scientific reports*, 5:15508–15508, 2014.

[7] Lucas Lacasa and Raul Toral. Description of stochastic and chaotic series using visibility graphs. *Physical Review E*, 82(3):036120, 2010.

[8] Bartolo Luque, Lucas Lacasa, Fernando Ballesteros, and Jordi Luque. Horizontal visibility graphs: Exact results for random time series. *Physical Review E*, 80(4):046103, 2009.

[9] Rogier Noldus and Piet Van Mieghem. Assortativity in complex networks. *Journal of Complex Networks*, page cnv005, 2015.

[10] Juliet Penrice, EB Cady, Ann Lorek, Marzena Wylezinska, PN Amess, RF Aldridge, Ann Stewart, JS Wyatt, and EOR Reynolds. Proton magnetic resonance spectroscopy of the brain in normal preterm and term infants, and early changes after perinatal hypoxia-ischemia. *Pediatric research*, 40(1):6–14, 1996.

[11] AB Rowley, SJ Payne, I Tachtsidis, MJ Ebden, JP Whiteley, DJ Gavaghan, L Tarassenko, M Smith, CE Elwell, and DT Delpy. Synchronization between arterial blood pressure and cerebral oxyhaemoglobin concentration investigated by wavelet cross-correlation. *Physiological measurement*, 28(2):161, 2006.

[12] Felix Scholkmann, Sonja Spichtig, Thomas Muehlemann, and Martin Wolf. How to detect and reduce movement artifacts in near-infrared imaging using moving standard deviation and spline interpolation. *Physiological measurement*, 31(5):649, 2010.

[13] Seetha Shankaran, Abbot R Laptook, Richard A Ehrenkranz, Jon E Tyson, Scott A McDonald, Edward F Donovan, Avroy A Fanaroff, W Kenneth Poole, Linda L Wright, Rosemary D Higgins, et al. Whole-body hypothermia for neonates with hypoxic–ischemic encephalopathy. *New England Journal of Medicine*, 353(15):1574–1584, 2005.

[14] Colin Stephen. Dynamic phase and group detection in pedestrian crowd data using multiplex visibility graphs. *Procedia Computer Science*, 53:410–419, 2015.

[15] Robert C Vannucci. Hypoxic-ischemic encephalopathy. *American journal of perinatology*, 17(03):113–120, 2000.

List of Figures